Inorganic Chemistry

Article

pubs.acs.org/IC

Mediator Enhanced Water Oxidation Using $Rb_4[Ru^{II}(bpy)_3]_5[\{Ru^{III}_4O_4(OH)_2(H_2O)_4\}(\gamma\text{-}SiW_{10}O_{36})_2]$ Film Modified Electrodes

Si-Xuan Guo,[†] Chong-Yong Lee,[†] Jie Zhang,*[,†] Alan M. Bond,*[,†] Yurii V. Geletii,[‡] and Craig L. Hill*[,‡]

[†]School of Chemistry, Monash University Clayton, Victoria 3800, Australia

[‡]Department of Chemistry, Emory University Dickey Drive 1515 Atlanta, Georgia 30322, United States

Supporting Information

ABSTRACT: The water insoluble complex $Rb_4[Ru^{II}(bpy)_3]_5[\{Ru^{III}_4O_4(OH)_2(H_2O)_4\}(\gamma\text{-}SiW_{10}O_{36})_2]$, ($[Ru^{II}bpy]_5[Ru^{III}_4POM]$), was synthesized from $Rb_8K_2[\{Ru^{IV}_4O_4(OH)_2(H_2O)_4\}(\gamma\text{-}SiW_{10}O_{36})_2]$ and used for electrocatalytic water oxidation under both thin- and thick-film electrode conditions. Results demonstrate that the $[Ru^{II}bpy]_5[Ru^{III}_4POM]$ modified electrode enables efficient water oxidation to be achieved at neutral pH using thin-film conditions, with $[Ru(bpy)_3]^{3+}$($[Ru^{III}bpy]$) acting as the electron transfer mediator and $[Ru^{V}_4POM]$ as the species releasing O_2. The rotating ring disc electrode (RRDE) method was used to quantitatively determine the turnover frequency (TOF) of the catalyst, and a value of 0.35 s^{-1} was obtained at a low overpotential of 0.49 V (1.10 V vs Ag/AgCl) at pH 7.0. The postulated mechanism for the mediator enhanced catalytic water process in a pH 7 buffer containing 0.1 M $LiClO_4$ as an additional electrolyte includes the following reactions (ion transfer for maintaining charge neutrality is omitted for simplicity): $[Ru^{II}bpy]_5[Ru^{III}_4POM] \rightarrow [Ru^{III}bpy]_5[Ru^{V}_4POM] + 13\ e^-$ and $[Ru^{III}bpy]_5[Ru^{V}_4POM] + 2H_2O \rightarrow [Ru^{III}bpy]_5[Ru^{IV}_4POM] + O_2 + 4H^+$. The voltammetry of related water insoluble $[Ru^{II}bpy]_2[S_2M_{18}O_{62}]$ (M = W and Mo) and $[Fe^{II}Phen]_x[Ru^{III}_4POM]$ materials has also been studied, and the lack of electrocatalytic water oxidation in these cases supports the hypothesis that $[Ru^{III}bpy]$ is the electron transfer mediator and $[Ru^{V}_4POM]$ is the species responsible for oxygen evolution.

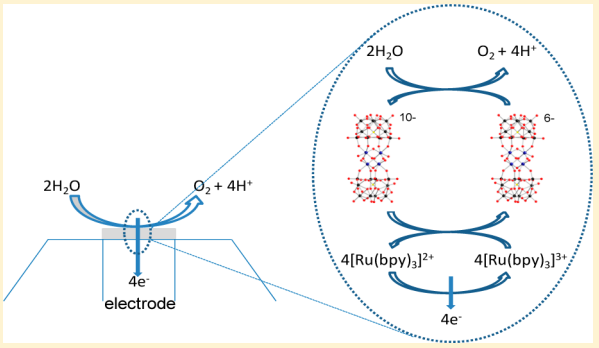

INTRODUCTION

Molecular hydrogen is a clean fuel that can be produced by the electrolysis of water. With suitable electrodes, oxygen may be evolved at the anode (eq 1) and hydrogen at the cathode (eq 2).

$$2H_2O \rightarrow O_2\uparrow + 4H^+ + 4e^- \quad (1)$$

$$2H^+ + 2e^- \rightarrow H_2\uparrow \quad (2)$$

The overall process (eq 3) is thermodynamically unfavorable by 1.24 V at 25 °C under standard conditions, and both half-cell reactions are usually slow in the absence of catalysts.

$$2H_2O \rightleftharpoons O_2\uparrow + 2H_2\uparrow \quad (3)$$

Water oxidation is the more kinetically demanding process and gives rise to a large part of the overpotential. Consequently, catalysts that allow electrochemical oxidation of water at a low overpotential are of great interest. Recently, many catalysts have been developed to minimize the overpotential.[1] In nature, the oxygen evolving center in Photosystem II catalyzes water oxidation with an overpotential equivalent to around 0.3 V, a turnover number (TON) was estimated to be as high as 6×10^5,[1c] and a turnover frequency (TOF) of about 10^3 s^{-1}.[1d] Catalysts with high efficiency, long-term stability, and low cost, which make them suitable for large-scale water electrolysis, have been sought by mimicking nature.[1,2] In addition to these biologically inspired systems, tailored metal containing synthetic catalysts that exhibit a series of electron transfer and proton coupled processes over a narrow potential range have been used to achieve water oxidation with a minimal overpotential.

Investigation of structure−activity relationships is now recognized as critical in the systematic development of effective water oxidation catalysts. In this context, polyoxometalates (POMs), a class of anionic clusters with frameworks built from transition metal oxo anions, provide distinct advantages because of their rich redox chemistry based on coupled electron and proton transfer, catalytic activity, and photoactivity.[3] Encapsulation of transition metals in the POM framework can change the redox chemistry and enhance the catalytic properties of the POM. In particular, incorporation of ruthenium has attracted

Received: April 14, 2014
Published: July 7, 2014

   dx.doi.org/10.1021/ic500878w | Inorg. Chem. 2014, 53, 7561−7570

attention due to its extensive redox and catalytic chemistry. For example, recently, Hill and co-workers[4,5] synthesized a POM with an embedded tetra-ruthenium(IV)-oxo core, $Rb_8K_2[\{Ru^{IV}_4O_4(OH)_2(H_2O)_4\}(\gamma\text{-}SiW_{10}O_{36})_2]$, which is a very effective molecular water oxidation catalyst. Simultaneously, Bonchio and co-workers synthesized the cesium salt of the same anion by another synthetic route.[6] This POM has four ruthenium centers that reside in a slightly distorted tetrahedron and are stabilized by hydroxo and oxo ligands. Unlike many other POMs, this compound is stable over a wide pH range, including highly acidic 0.5 M H_2SO_4.[7]

Hill et al.[4] used $[Ru(bpy)_3]^{3+}$ as the sacrificial electron acceptor for $[\{Ru^{IV}_4O_4(OH)_2(H_2O)_4\}(\gamma\text{-}SiW_{10}O_{36})_2]^{10-}$-catalyzed oxidation of water at pH 7 with a TON of 18 (mol O_2/mol Ru-POM). Sartorel et al.[6] used Ce^{4+} as the sacrificial electron acceptor for $[\{Ru^{IV}_4O_4(OH)_2(H_2O)_4\}(\gamma\text{-}SiW_{10}O_{36})_2]^{10-}$-catalyzed oxidation of water in an acidic medium (pH 0.6) with a TOF of 0.13 s^{-1}. Bonchio and coauthors have attached $[\{Ru^{IV}_4O_4(OH)_2(H_2O)_4\}(\gamma\text{-}SiW_{10}O_{36})_2]^{10-}$ to multiwalled carbon nanotubes functionalized with positively charged polyamidoamine (PAMAM) ammonium dendrimers and realized electrocatalytic water oxidation at pH 7 with a TOF of 0.085 s^{-1} at an overpotential of 0.60 V.[8] The catalytic activity of $[\{Ru^{IV}_4O_4(OH)_2(H_2O)_4\}(\gamma\text{-}SiW_{10}O_{36})_2]^{10-}$ is significantly improved when dendron functionalized graphene is chosen as the support for catalyst immobilization.[9] We have recently immobilized $[\{Ru^{IV}_4O_4(OH)_2(H_2O)_4\}(\gamma\text{-}SiW_{10}O_{36})_2]^{10-}$ on a wet graphene modified electrode, and achieved a TOF of 0.82 s^{-1} in pH 7.50 buffer at high ionic strength at an overpotential as low as 0.35 V.[10]

To establish whether high catalytic efficiency could be achieved at low overpotential, we adopted an electrode modification approach based on that employed in commercially successful glucose enzyme electrodes. In the glucose biosensor, an electron transfer mediator is frequently used to facilitate the electron transfer between glucose oxidase and the electrode.[11] That is, the mediator is oxidized electrochemically to give a product that oxidizes the glucose oxidase enzyme and recovers the mediator to give a reaction scheme that achieves catalysis of the oxidation of the substrate, glucose. This approach also has been used by Anson et al. for catalytic reduction of O_2 by cobalt(II) tetrakis(4-*N*-methylpyridy1)porphyrin mediated by the $[Ru(NH_3)_6]^{3+/2+}$ reaction at Nafion-coated electrodes.[12] Inspired by these studies, we report that electrodes modified with water insoluble $Rb_4[Ru(bpy)_3]_5[\{Ru^{III}_4O_4(OH)_2(H_2O)_4\}(\gamma\text{-}SiW_{10}O_{36})_2]$ ($[Ru^{II}bpy]_5[Ru^{III}_4POM]$) films have now been developed for the electrocatalytic oxidation of water, where the oxidized form of the counter cation $[Ru(bpy)_3]^{3+}$ ($[Ru^{III}bpy]$) serves as an electron transfer mediator. This approach differs from that reported by Anson et al.,[12] where the mediator and catalyst are derived from different compounds.

Bond and co-workers already have synthesized water insoluble $[Ru^{II}bpy]$ complexes of $[S_2Mo_{18}O_{62}]^{4-}$, $[S_2W_{18}O_{62}]^{4-}$, and $[\alpha\text{-}SiW_{12}O_{40}]^{4-}$ and showed that they exhibit attractive photocatalytic and electrocatalytic properties.[13,14] Importantly, if both the Ru-based mediator and the POM catalyst are aligned in close proximity in a solid-state thin-film form, it is postulated that electron transfer will be facilitated and mass transport limitations encountered in bimolecular reactions in solution will be minimized. Under these circumstances, the catalytic efficiency of $[\{Ru^{V}_4O_4(OH)_2(H_2O)_4\}(\gamma\text{-}SiW_{10}O_{36})_2]^{6-}$ should be substantial at low overpotential, as demonstrated in this study. The rotating ring disc electrode (RRDE)[15] method has been used to determine the TOF values. This technique has been used by Murray et al. for the measurement of O_2 generated from a catalytic water oxidation reaction.[16]

EXPERIMENTAL SECTION

Reagents. The following chemicals were used as received: $[Ru(bpy)_3]Cl_2$ (ruthenium-tris(2,2′-bipyridyl)dichloride) and $NaBH_4$ from Sigma-Aldrich, Na_2HPO_4 and NaH_2PO_4 (Fluka, AR grade), $LiClO_4$ (AR grade, BDH), H_2SO_4 (AR grade, Univar), KPF_6 (Aldrich), Nafion, ruthenium red, RuO_2, and iron phenanthroline (Sigma-Aldrich). $Rb_8K_2[\{Ru^{IV}_4O_4(OH)_2(H_2O)_4\}(\gamma\text{-}SiW_{10}O_{36})_2]$ was synthesized according to a procedure in literature.[4] Deionized water from a MilliQ–MilliRho purification system (resistivity 18 MΩ·cm) was used to prepare all aqueous electrolyte solutions. Buffer solutions were prepared by mixing 0.1 M Na_2HPO_4 and 0.1 M NaH_2PO_4 solutions and adjusting the pH to the desired value, which was measured using a Mettler-Toledo SevenCompact S220-BIO pH/ion meter equipped with an InLab Routine Pro-ISM sensor (Mettler-Toledo, Greifensee, Switzerland). For 0.1 M buffer solutions containing 0.1 M additional electrolyte, the pH was adjusted to 7.0 in all cases.

Synthesis of $Rb_4[Ru^{II}bpy]_5[Ru^{III}_4POM]$, ($[Ru^{II}bpy]_5[Ru^{III}_4POM]$), and Other $[Ru^{II}bpy]$ Complexes. To prepare the water insoluble $[Ru^{II}bpy]$-$[\{Ru^{III}_4O_4(OH)_2(H_2O)_4\}(\gamma\text{-}SiW_{10}O_{36})_2]^{14-}$ complexes, we first reduced $Rb_8K_2[\{Ru^{IV}_4O_4(OH)_2(H_2O)_4\}(\gamma\text{-}SiW_{10}O_{36})_2]$ to $[\{Ru^{III}_4O_4(OH)_2(H_2O)_4\}(\gamma\text{-}SiW_{10}O_{36})_2]^{14-}$ by adding 5 mM of $NaBH_4$ to 0.5 mM of $Rb_8K_2[\{Ru^{IV}_4O_4(OH)_2(H_2O)_4\}(\gamma\text{-}SiW_{10}O_{36})_2]$. $[Ru(bpy)_3]Cl_2$ (4 mM) was then added to the solution. The precipitated solid was collected by centrifugation, purified by redispersing in water, and then collected after centrifugation, before finally drying overnight under vacuum. RDE voltammetry was used to establish the oxidation state of the Ru centers after the reduction of $[\{Ru^{IV}_4O_4(OH)_2(H_2O)_4\}(\gamma\text{-}SiW_{10}O_{36})_2]^{10-}$ by a 10-fold excess of $NaBH_4$ under a N_2 atmosphere. Ten minutes after the $NaBH_4$ addition, 0.14 mL of concentrated H_2SO_4 was added to the solution (5 mL) to adjust the final concentration of H_2SO_4 to 0.5 M. RDE voltammograms were obtained immediately. These results proved that all Ru(IV) atoms were reduced to Ru(III) (vide infra). Elemental analysis gave C, 19.70; N, 4.42; and H, 1.85% versus C, 20.01; N, 4.69; and H, 1.83% as predicted for $Rb_4[Ru(bpy)_3]_5[\{Ru^{III}_4O_4(OH)_2(H_2O)_4\}(\gamma\text{-}SiW_{10}O_{36})_2]\cdot xH_2O$ ($x \approx 17$). The number of water molecules represents the best fit of elemental analysis data but is subject to considerable uncertainty. Energy-dispersive X-ray spectroscopy (EDX) results show the presence of rubidium. The average weight ratio of 0.246 for Ru/W equates to 9 Ru atoms per 20 W atoms. This result is consistent with a $[Ru^{II}bpy]$/$[Ru^{III}_4POM]$ ratio of 5:1. No potassium or sodium was detected. ICP-OES (Varian 720) analysis gives a ratio of 4.2:9.0:19.5 for Rb/Ru/W, which is very close to the ratio of 4:9:20 predicted for $Rb_4[Ru(bpy)_3]_5[\{Ru^{III}_4O_4(OH)_2(H_2O)_4\}(\gamma\text{-}SiW_{10}O_{36})_2]$. For convenience, and because Rb^+ exchange probably occurs with electrolyte cation in the electrochemical studies, the solid is referred to as $[Ru^{II}bpy]_5[Ru^{III}_4POM]$ henceforth in this Article.

Water insoluble $[Ru^{II}bpy]_x[Ru^{IV}_4POM]$ and $[Fe^{II}Phen]_x[Ru^{III}_4POM]$ materials were synthesized using a similar approach. EDX results for $[Ru^{II}bpy]_x[Ru^{IV}_4POM]$ material again showed the presence of a small quantity of rubidium. The average weight ratio of 0.221 for Ru/W equates to 8 Ru atoms vs 20 W atoms, or a $[Ru^{II}bpy]$/$[Ru^{IV}_4POM]$ ratio of 4:1, which indicates that the material is $Rb_2[Ru^{II}bpy]_4[Ru^{IV}_4POM]$. Again, no potassium or sodium was detected. This material is referred to as $[Ru^{II}bpy]_4[Ru^{IV}_4POM]$ in the rest of this Article.

The known compounds $[Ru(bpy)_3]_2[S_2Mo_{18}O_{62}]$ and $[Ru(bpy)_3]_2[S_2W_{18}O_{62}]$ were synthesized by adding $[Ru(bpy)_3]Cl_2$ (4 mM) to a solution containing 0.5 mM of the relevant anion,[11] followed by purification and drying as for $[Ru^{II}bpy]_5[Ru^{III}_4POM]$.

dx.doi.org/10.1021/ic500878w | Inorg. Chem. 2014, 53, 7561−7570

Preparation of Modified Electrodes. The electrodes modified with $[Ru^{II}bpy]_5[Ru^{III}{}_4POM]$ were prepared by dispersing the solid in water and then drop-casting 5 μL of the slurry onto the electrode surface and allowing it to dry at room temperature. Two loadings were used. For a thin-film modified electrode, the coating solution contained 0.16 mg mL^{-1} of $[Ru^{II}bpy]_5[Ru^{III}{}_4POM]$, and for thick-film modified electrodes, the coating solution contained 8.0 mg mL^{-1} of the solid. For preparation of the $[Ru^{II}bpy]_4[Ru^{IV}{}_4POM]$ and $[Fe^{II}Phen]_x[Ru^{III}{}_4POM]$, $[Ru^{II}bpy]_2[S_2Mo_{18}O_{62}]$ and $[Ru^{II}bpy]_2[S_2W_{18}O_{62}]$ modified electrodes, the coating solutions contained the same molar concentration of POM as used for preparation of the $[Ru^{II}bpy]_5[Ru^{III}{}_4POM]$ thick-film modified electrodes. In RRDE (Pt ring, glassy carbon (GC) disk) studies, $[Ru^{II}bpy]_5[Ru^{III}{}_4POM]$ modified electrodes were coated with 3 μL of 0.02% Nafion solution to improve the adhesion of the film to the electrode surface.

Electrochemistry. Voltammograms were acquired at 22 ± 2 °C using a CHI 760D electrochemical workstation (CH Instruments, Austin, TX). A standard three-electrode electrochemical cell arrangement was employed using a GC (3.0 mm diameter, CH Instruments, Austin, TX) working electrode, a Pt wire counter electrode, and a Ag/AgCl (3 M NaCl) reference electrode (0.210 V vs SHE).[17] The effective areas of the macrodisk GC and Pt electrodes were determined by measuring the reduction of 1.0 mM $[Fe(CN)_6]^{3-}$ as $K_3[Fe(CN)_6]$ in water (0.5 M KCl) by cyclic voltammetry and using the Randle–Sevcik equation with a known diffusion coefficient of 7.6×10^{-6} cm^2 s^{-1} for $[Fe(CN)_6]^{3-}$.[18] For RRDE and rotating disk electrode (RDE) studies, a rotating ring disk electrode rotator (RRDE-3A, ALS Co., Japan) was connected to the electrochemical workstation. A GC disk (4.0 mm diameter)–Pt ring (5.0 mm i.d./7.0 mm o.d., ALS Co., Ltd., Japan) working electrode was used for RRDE studies, while a GC disk (3.0 mm diameter, ALS Co., Japan) or a Pt disk (3.0 mm diameter, ALS Co., Ltd., Japan) working electrode was used for RDE studies, along with the same reference and auxiliary electrodes employed in the voltammetry. The collection efficiency of the RRDE[16] was measured using 1.0 mM $[Fe(CN)_6]^{3-}$ (0.1 M sodium phosphate buffer, pH 7.0, and 0.1 M $LiClO_4$), and calculated to be 0.42. The working electrodes in all experiments were polished with an aqueous slurry of 0.3 μm alumina, cleaned with deionized water, sonicated, rinsed with water, and then dried under nitrogen. The solution was purged with nitrogen for at least 15 min before measurement, and then the electrochemical cell was kept under a positive pressure of nitrogen at all times.

Simulations of cyclic voltammograms were carried out with DigiSim (Version 3.05) software.[19]

RESULTS AND DISCUSSION

Voltammetry of $[\{Ru^{IV}{}_4O_4(OH)_2(H_2O)_4\}(\gamma\text{-}SiW_{10}O_{36})_2]^{10-}$ in Aqueous Solutions. Previous studies in our laboratories have shown that the voltammetry of $[\{Ru^{IV}{}_4O_4(OH)_2(H_2O)_4\}(\gamma\text{-}SiW_{10}O_{36})_2]^{10-}$ in aqueous solutions is strongly pH dependent.[7] In 0.5 M H_2SO_4 medium, both the cyclic and RDE voltammograms obtained for $[\{Ru^{IV}{}_4O_4(OH)_2(H_2O)_4\}(\gamma\text{-}SiW_{10}O_{36})_2]^{10-}$ show two one-electron $Ru^{IV/V}$ processes with $E^{\circ\prime}$ (defined as $(E_p^{ox} + E_p^{red})/2$) values of +869 and +1057 mV, where E_p^{ox} and E_p^{red} are oxidation and reduction peak potentials, respectively; four successive one-electron $Ru^{IV/III}$ processes at around +621, +475, +255, and +202 mV; and a multielectron reduction process at −346 mV, which is associated with reduction of the polytungstate framework (Figure 1). Two further $Ru^{IV/V}$ oxidation processes were also detected at very positive potentials by FT ac voltammetry.[7]

At neutral pH, well-defined voltammograms can only be obtained in the presence of high concentrations of additional electrolyte.[7] It was postulated that the electrical double layer suppresses the rate of electron transfer.

RDE Voltammetry in Aqueous 0.5 M H_2SO_4 Solution of the Product Produced by Reduction of $Rb_8K_2[\{Ru^{IV}{}_4O_4(OH)_2(H_2O)_4\}(\gamma\text{-}SiW_{10}O_{36})_2]$ with $NaBH_4$. RDE voltammetric experiments were carried out to establish the oxidation states of the Ru centers in the product formed when 0.5 mM $[\{Ru^{IV}{}_4O_4(OH)_2(H_2O)_4\}(\gamma\text{-}SiW_{10}O_{36})_2]^{10-}$ solution was reduced by an excess of $NaBH_4$ (5 mM) (see Experimental Section for details). The RDE voltammogram of 0.5 mM $[\{Ru^{IV}{}_4O_4(OH)_2(H_2O)_4\}(\gamma\text{-}SiW_{10}O_{36})_2]^{10-}$ solution (0.5 M H_2SO_4) (Figures 1b and 2) shows a zero-current region at a potential of about +750 mV and two oxidation and five reduction processes (including one tungsten framework based multielectron process).[7] After the addition of $NaBH_4$, the zero-current region shifts to around 0 V. A total of six oxidation and the multielectron reduction processes are now observed (Figure 2). This confirms that $NaBH_4$ reduces all four Ru(IV) centers to Ru(III). Further addition of $NaBH_4$ does not change the RDE voltammograms, indicating that $NaBH_4$ does not reduce the tungsten polyoxometalate framework or reduce the Ru(III) centers to Ru(II).

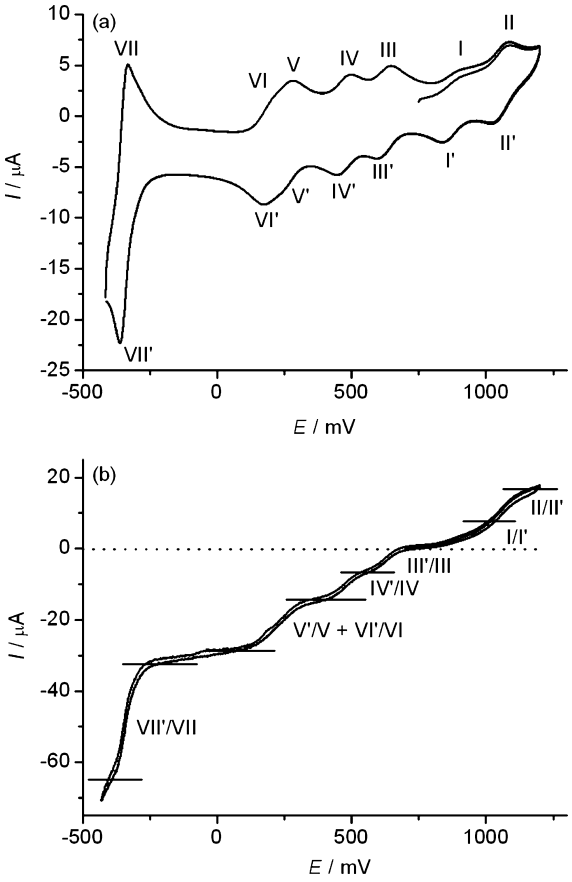

Figure 1. Cyclic (a) and RDE (b) voltammograms of 0.5 mM $Rb_8K_2[\{Ru^{IV}{}_4O_4(OH)_2(H_2O)_4\}(\gamma\text{-}SiW_{10}O_{36})_2]$ at a glassy carbon electrode in 0.5 M H_2SO_4. For the cyclic voltammogram, the scan rate is 50 mV s^{-1}. For the RDE voltammogram, the rotation rate is 104.7 rad s^{-1}, and the scan rate is 10 mV s^{-1}.

Voltammetry of $[Ru^{II}bpy]_5[Ru^{III}{}_4POM]$ Films in 0.5 M H_2SO_4. The electrochemistry of a $[Ru^{II}bpy]_5[Ru^{III}{}_4POM]$-coated GC electrode also was studied in aqueous 0.5 M H_2SO_4 solution. At a thin-film modified electrode, only one surface-confined oxidation process was observed with an $E^{\circ\prime}$ value (midpoint potential E_m again assumed to be equal to $E^{\circ\prime}$) of +1065 mV for the first cycle and +1049 mV for second and subsequent cycles (Figure 3a). The analogs of the solution phase series of one electron processes associated with oxidation

dx.doi.org/10.1021/ic500878w | Inorg. Chem. 2014, 53, 7561–7570

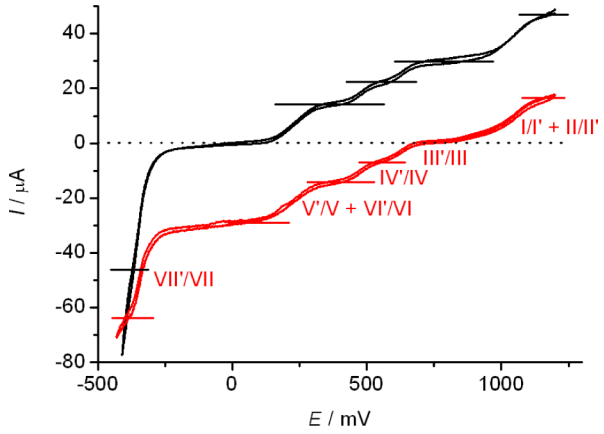

Figure 2. RDE voltammograms obtained with a 0.5 mM $[\{Ru^{IV}_4O_4(OH)_2(H_2O)_4\}(\gamma\text{-}SiW_{10}O_{36})_2]^{10-}$ solution (0.5 M H_2SO_4) (red line) before and (black line) after the addition of 5 mM $NaBH_4$.

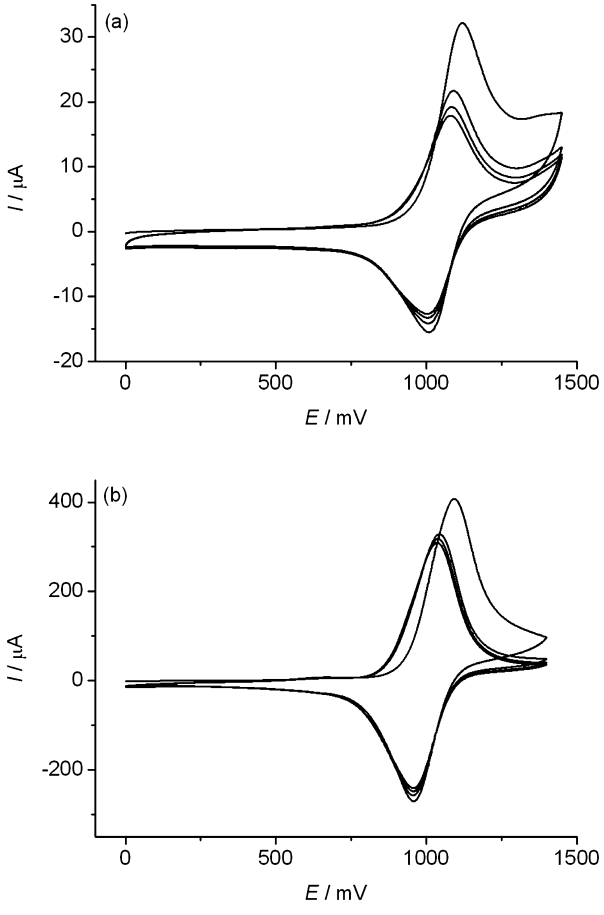

Figure 3. Cyclic voltammograms obtained with (a) thin- and (b) thick-film $[Ru^{II}bpy]_5[Ru^{III}_4POM]$ modified GC electrodes in 0.5 M H_2SO_4. Scan rate: 100 mV s^{-1}.

of $[Ru^{III}_4POM]$ are essentially absent. $[Ru^{IV}_4POM]$ has been immobilized on graphene[10] and polyethylenimine[20] and has shown well-defined voltammograms when in contact with acidic solutions. However, in the case of $[Ru^{II}bpy]_5[Ru^{III}_4POM]$, presumably the $[Ru^{III}_4POM]$ processes are inhibited by the presence of the $[Ru^{II}bpy]$ cation, and thus, $[Ru^{III}bpy]$ acts as the electron transfer mediator for the oxidation of $[Ru^{III}_4POM]$ at slightly more positive potentials than 1000 mV to give a multielectron process. The overall underlying electrode reactions giving the multielectron process are summarized by eqs 4–8 for the first voltammetric sweep, taking into account the known reversible potentials for both $[Ru^{II}bpy]/[Ru^{III}bpy]$ (1.06 V vs Ag/AgCl[21]) and $[Ru^{III}_4POM]$ oxidation:[7]

$$[Ru^{II}bpy]_5[Ru^{III}_4POM] \rightleftharpoons [Ru^{III}bpy]_5[Ru^{III}_4POM] + 5e^- \quad (4)$$

$$[Ru^{III}bpy]_5[Ru^{III}_4POM] \rightarrow [Ru^{II}bpy]_5[Ru^{V}Ru^{IV}_3POM] \quad (5)$$

$$[Ru^{II}bpy]_5[Ru^{V}Ru^{IV}_3POM] \rightleftharpoons [Ru^{III}bpy]_5[Ru^{V}Ru^{IV}_3POM] + 5e^- \quad (6)$$

$$[Ru^{III}bpy]_5[Ru^{V}Ru^{IV}_3POM] \rightarrow [Ru^{II}bpy][Ru^{III}bpy]_4[Ru^{V}_2Ru^{IV}_2POM] \quad (7)$$

$$[Ru^{II}bpy][Ru^{III}bpy]_4[Ru^{V}_2Ru^{IV}_2POM] \rightleftharpoons [Ru^{III}bpy]_5[Ru^{V}_2Ru^{IV}_2POM] + e^- \quad (8)$$

The surface-confined electron transfer reactions (eqs 4, 6, and 8) also must involve the ingress and egress of ions into or out of the film (e.g., the uptake of anions HSO_4^- and SO_4^{2-} or the loss of cations Rb^+ and H^+) to maintain charge neutrality, a process which is omitted here and in the rest of this Article for simplicity. On the basis of reversible potentials in acidic solutions,[7] $[Ru^{III}bpy]$ is thermodynamically capable of accepting two electrons from $[Ru^{IV}_4POM]$. Therefore, $[Ru^{V}_2Ru^{IV}_2POM]$ is the highest oxidation state accessible in the film.

In the first cycle of potential, the peak area associated with the multielectron oxidation process is significantly larger than that of the companion reduction component due to the contribution from the initial oxidation of $[Ru^{III}_4POM]$ to $[Ru^{V}_2Ru^{IV}_2POM]$ by $[Ru^{III}bpy]$ (eqs 5 and 7). Because the reactions in eqs 5 and 7 are irreversible, their contribution is diminished in the second and subsequent cycles of potential due to $[Ru^{III}_4POM]$ depletion from the film. Eventually, from the second scan, the reaction in eq 9 takes place:

$$[Ru^{II}bpy]_5[Ru^{V}_2Ru^{IV}_2POM] \rightleftharpoons [Ru^{III}bpy]_5[Ru^{V}_2Ru^{IV}_2POM] + 5e^- \quad (9)$$

This proposed reaction mechanism (eqs 4–9) is supported by the simulated results (Figure S1, Supporting Information) obtained from a similar but simplified mechanism, which demonstrates a qualitative agreement with the experimental data (Figure 3).

At a thick-film modified electrode (Figure 3b), the current magnitude is much larger and only a single oxidation process is detected with a midpoint potential of +1025 mV (first cycle) and +1000 mV (second and subsequent cycles). The potential for this process is similar to that found in the thin-film case. In essence, the same reactions described in eqs 4–9 are proposed to occur. The voltammograms obtained with multiple cycling of potentials are constant after the initial cycle which indicates that the thick-film configuration is stable.

The shapes of voltammograms in Figure 3 imply that the electrooxidation of $[Ru^{II}bpy]_5[Ru^{III}_4POM]$ (eqs 4–8) does not give rise to any significant catalytic oxidation of water under either thin- or thick-film conditions when 0.5 M H_2SO_4 is the

dx.doi.org/10.1021/ic500878w | Inorg. Chem. 2014, 53, 7561–7570

electrolyte. This is expected because $[Ru^{V}_{2}Ru^{IV}_{2}POM]$ is not the catalytically active form for water oxidation in acidic media.[7b]

The charge associated with oxidation in Figure 3 (the second and subsequent cycles of potential) for the surface-confined process (eq 9) was obtained by integration. The quantity of $[Ru^{II}bpy]_5[Ru^{III}_{4}POM]$ confined to the surface was then calculated on the basis of Faraday's Law, assuming the number of electrons transferred per $[Ru^{II}bpy]_5[Ru^{III}_{4}POM]$ moiety is 5 (based on eq 9). In the thick-film case, the lack of efficient film-to-electrode communication, due to slow coupled charge neutralization through ion partition, may restrict the extent of oxidation. However, assuming n = 5, the loadings of $[Ru^{II}bpy]_5[Ru^{III}_{4}POM]$ were calculated to be 1.3×10^{-9} and 1.5×10^{-8} mol cm^{-2} for the thin- and thick-films, respectively. These values correspond to the oxidation of fractions of 1.0 and 0.23 of the values estimated from the known mass of $[Ru^{II}bpy]_5[Ru^{III}_{4}POM]$ introduced onto the electrode surfaces. This result implies that the communication between the electrode and $[Ru^{II}bpy]_5[Ru^{III}_{4}POM]$ is excellent in the thin-film case and reasonable for the thick-film.

The cyclic voltammetry of a thick-film $[Ru^{II}bpy]_4[Ru^{IV}_{4}POM]$ modified electrode in 0.5 M H_2SO_4 electrolyte is very similar to that of thick-film $[Ru^{II}bpy]_5[Ru^{III}_{4}POM]$ modified electrode (compare Figure 3 and Figure S2 in the Supporting Information). Thus, a single oxidation process is again found with an E_m value of +1090 mV for the first cycle and +1052 mV for second and subsequent cycles. The latter value is about 52 mV more positive than that found on second and subsequent cycles with the thick-film $[Ru^{II}bpy]_5[Ru^{III}_{4}POM]$ modified electrode (Figure 3b), implying that the charge neutralization process is less favorable. Furthermore, in this case, the peak current decreases rapidly on multiple cycling of the potential (Figure S2, Supporting Information). This suggests that the $[Ru^{II}bpy]_4[Ru^{IV}_{4}POM]$ film is less stable (more soluble) in this acidic medium. However, the mechanism associated with the voltammetric process is similar in both cases, as would be expected.

Voltammetry of $[Ru^{II}bpy]_5[Ru^{III}_{4}POM]$ Films in 0.1 M $LiClO_4$ (Unbuffered) Solution. In addition, the voltammetry of both thick- and thin-film chemically modified $[Ru^{II}bpy]_5[Ru^{III}_{4}POM]$ glassy carbon electrodes was studied in an unbuffered solution containing 0.1 M $LiClO_4$ as the supporting electrolyte. The pH of this solution is about 5.5. Oxidation of the $[Ru^{II}bpy]_5[Ru^{III}_{4}POM]$ film on the electrode surface again requires ion transfer to maintain charge neutrality in the solid film phase. The hydrophobic anion ClO_4^- has often been found to be suitable for this purpose because it can transfer rapidly into solid films and inhibit film dissolution.[22] Data in Figure 4 provide evidence of weak catalytic current, particularly in the thin-film case at potentials where oxidation occurs, based on the diminished reversibility of the voltammetric response and by an increase in the current at positive potentials. However, long-term catalytic water oxidation is not favorable in an unbuffered solution because the generation of O_2 will be accompanied by a large H^+ concentration increase close to the electrode surface. This will significantly lower the pH near the electrode surface, which in turn would lead, in accordance with the pH dependent reversible potential for water oxidation, E°_{pH} (eq 10), to a significant positive shift in the reversible potential required for water oxidation, thereby inhibiting this process.

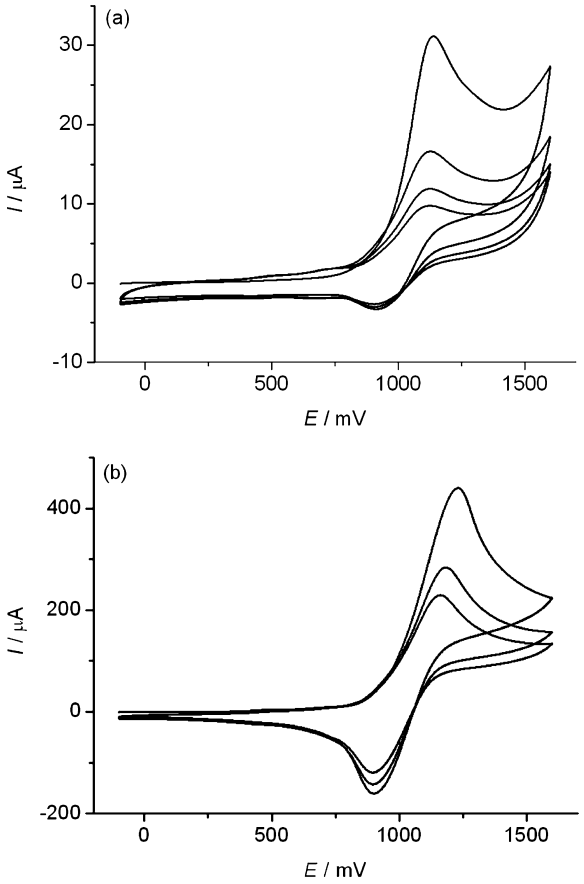

Figure 4. Cyclic voltammograms derived from (a) thin- and (b) thick-film $[Ru^{II}bpy]_5[Ru^{III}_{4}POM]$ modified GC electrodes with aqueous 0.1 M $LiClO_4$ as the supporting electrolyte. Scan rate: 100 mV s^{-1}.

$$E^{\circ}_{pH} = E^{\circ} - 0.059\ pH \qquad (10)$$

(where E° (1.24 V vs SHE or 1.02 V vs Ag/AgCl) is the reversible potential of water oxidation under standard unit activity conditions.) Consequently, to more efficiently oxidize water, a buffered electrolyte solution is preferred so that the thermodynamics of water oxidation can remain favorable even after the initial production of O_2. The E_m value with 0.1 M $LiClO_4$ as the electrolyte (pH = 5.5) is similar to that found with highly acidic 0.5 M H_2SO_4, as expected if this oxidation process corresponds to the $[Ru(bpy)_3]^{2+/3+}$ couple.

Voltammetry of $[Ru^{II}bpy]_5[Ru^{III}_{4}POM]$ Films in a 0.1 M Sodium Phosphate Buffer (pH 7.0) Containing 0.1 M $LiClO_4$ as an Additional Supporting Electrolyte. Chemically modified $[Ru^{II}bpy]_5[Ru^{III}_{4}POM]$ electrodes exhibit irreversible rather than close-to-chemically reversible oxidation when a phosphate buffer solution (pH 7.0) containing 0.1 M $LiClO_4$ is used as the electrolyte (Figure 5). Importantly, gas bubbles are now visually detected on the working electrode surface (Figure 6) when the potential is scanned to values more positive than 800 mV. Consequently, this irreversible oxidation process is now associated with water oxidation catalyzed by electrogenerated $[Ru^{III}bpy]_5[Ru^{V}_{4}POM]$ (see below). In the case of the thin-film configuration, this voltammetric process in pH 7 buffer containing 0.1 M $LiClO_4$ has a peak potential of +1093 mV, which is still similar to that without the buffer, but the peak current of about 70 μA is now significantly enhanced (Figure 5a). The peak potential is now approximately 490 mV more positive than the standard reversible potential for the

dx.doi.org/10.1021/ic500878w | Inorg. Chem. 2014, 53, 7561−7570

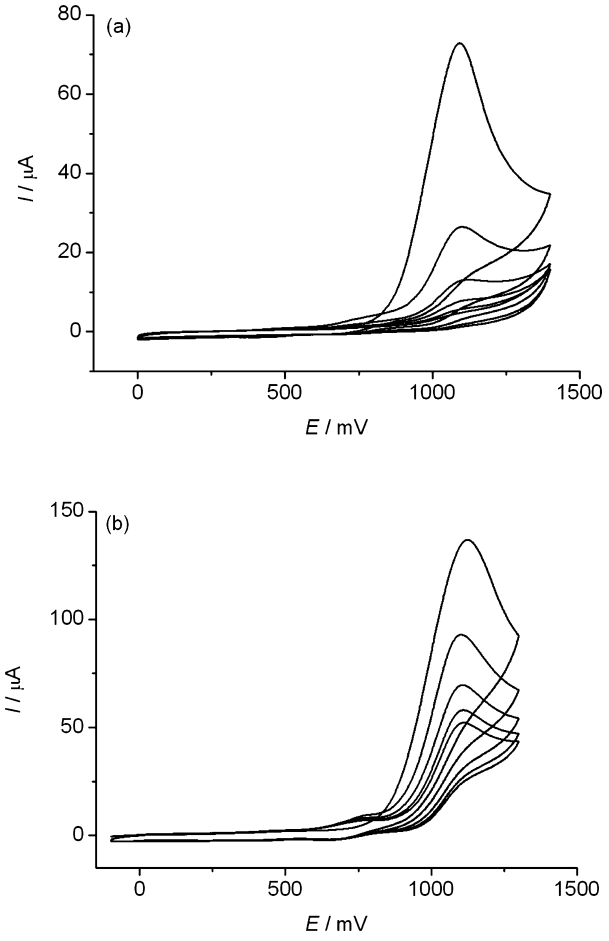

Figure 5. Cyclic voltammograms derived from (a) thin- and (b) thick-film $[Ru^{II}bpy]_5[Ru^{III}{}_4POM]$ modified GC electrodes with 0.1 M sodium phosphate buffer (pH 7.0) containing 0.1 M $LiClO_4$ as the additional supporting electrolyte. Scan rate: 50 mV s^{-1}.

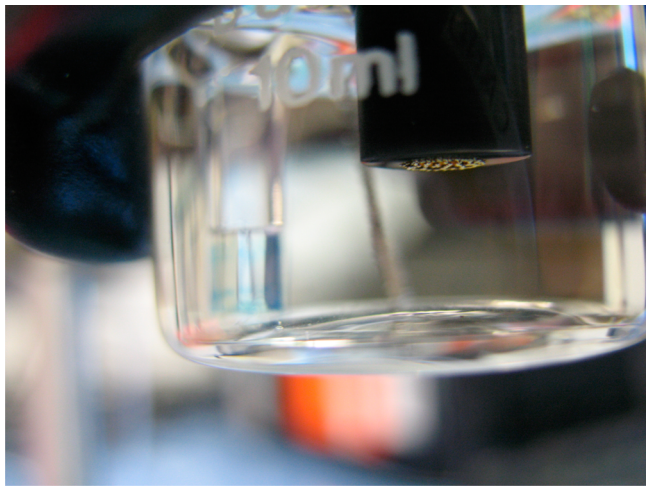

Figure 6. Photo taken after the potential was cycled five times between 0 and +1300 mV vs Ag/AgCl at a scan rate of 50 mV s^{-1} on a thin-film $[Ru^{II}bpy]_5[Ru^{III}{}_4POM]$ modified GC electrode with 0.1 M sodium phosphate buffer (pH 7.0) containing 0.1 M $LiClO_4$ as the additional supporting electrolyte.

oxidation of H_2O to O_2 at pH 7.0 (0.607 V vs Ag/AgCl) at 22 °C. The decrease in catalytic current on repetitive cycling of the potential (Figure 5) is likely to be due to blockage of the active sites by generated O_2 bubbles remaining adhered to the surface. This hypothesis is supported by the fact that the catalytic current could be recovered to about 95% of its initial value when the modified electrode without any applied potential was left in the electrolyte solution for 10 min after the initial generation of oxygen in the voltammetric experiment (Figure S3, Supporting Information), when time is available to allow gradual release of O_2 from the electrode surface active sites.

Under buffered pH 7.0 conditions, and unlike in 0.5 M H_2SO_4, complete oxidation of $[Ru^{III}{}_4POM]$ to $[Ru^{V}{}_4POM]$ by electrochemically generated $[Ru^{III}bpy]$ is now thermodynamically favorable on the basis of the known reversible potentials.[7,17] The overall solid-state electron transfer processes and the catalytic reaction involving $[Ru^{II}bpy]_5[Ru^{V}{}_4POM]$ that occur on the voltammetric time scale for the first voltammetric sweep therefore can be described by eqs 11 and 12.

$$[Ru^{II}bpy]_5[Ru^{III}{}_4POM] \rightarrow [Ru^{III}bpy]_5[Ru^{V}{}_4POM] + 13e^- \quad (11)$$

$$[Ru^{III}bpy]_5[Ru^{V}{}_4POM] + 2H_2O \rightarrow [Ru^{III}bpy]_5[Ru^{IV}{}_4POM] + O_2 + 4H^+ \quad (12)$$

In the electrooxidation of $[Ru^{II}bpy]_5[Ru^{III}{}_4POM]$ to form $[Ru^{III}bpy]_5[Ru^{V}{}_4POM]$ (eq 11), $[Ru^{III}{}_4POM]$ is oxidized to $[Ru^{V}{}_4POM]$ by $[Ru^{III}bpy]$ as an electron transfer mediator, similar to the process described in eqs 4–8 for the 0.5 M H_2SO_4 case. In eqs 4, 6, 8, and 11, it is assumed that $[Ru^{III}{}_4POM]$ is oxidized by the electrogenerated $[Ru^{III}bpy]$ on the basis of the evidence that direct electron transfer to the electrode is very slow.

In the case of the thick-film modified electrode, the peak current for the catalytic process is detected at +1100 mV with a peak current of about 140 μA (Figure 5b). This peak current value is only about twice that of the thin-film modified electrode under the same voltammetric conditions, even though the loading of $[Ru^{II}bpy]_5[Ru^{III}{}_4POM]$ is about 50 times that for the thin-film electrode. This further indicates that a thick-film configuration is not suitable for efficient electrocatalytic oxidation of water.

The addition of 0.1 M $LiClO_4$ electrolyte to the buffer solution is believed to facilitate rapid anion transfer to the solid-state $[Ru^{II}bpy]_5[Ru^{III}{}_4POM]$ film during its oxidation to form $[Ru^{II}bpy]_5[Ru^{V}{}_4POM]$ (eq 11) and hinder its dissolution. The use of 0.1 M KPF_6 electrolyte that also contains a hydrophobic anion (PF_6^-) gives similar voltammetric results when used with 0.1 M sodium phosphate buffer.

Molecular catalysts may not be stable under catalytic conditions, and very often, the decomposed products are the active forms of the catalysts.[23] It is well-known that RuO_2 is a good water oxidation electrocatalyst in both acidic and alkaline media.[24] To rule out the possibility that the catalytic water oxidation current resulted from RuO_2, a possible decomposition product of oxidized $[Ru^{II}bpy]_5[Ru^{III}{}_4POM]$, control experiments were undertaken using RuO_2 modified electrodes. In determining the amount of RuO_2 used for this controlled experiment, it was assumed that all Ru, including that associated with $[Ru^{II}bpy]$, was decomposed into RuO_2 in the highly positive potential region to give a worst-case scenario. The cyclic voltammetric result (Figure S4, Supporting Information) shows that the current decreases rapidly upon cycling of the potential, suggesting that the RuO_2 film is unstable. This poor

dx.doi.org/10.1021/ic500878w | Inorg. Chem. 2014, 53, 7561–7570

stability, not observed in the case of $[Ru^{II}bpy]_5[Ru^{III}_4POM]$ modified electrode, may be attributed to the fact that the rapid ion transfer required to maintain charge neutrality in the RuO_2 film has to be achieved via H^+ or OH^-,[25] which is difficult in neutral media. Furthermore, unlike the case with the $[Ru^{II}bpy]_5[Ru^{III}_4POM]$ modified electrode (Figure 5), no oxygen gas bubbles were visible to the unaided eye, and the voltammetric characteristics differ (compare Figure 5 and Figure S3 in the Supporting Information). All the evidence suggests that the catalytic activity of $[Ru^{II}bpy]_5[Ru^{III}_4POM]$ toward water oxidation is not due to RuO_2 formed as a decomposition product.

The voltammetry of a $[Ru^{II}bpy]_4[Ru^{IV}_4POM]$ thick-film modified electrode was also studied in 0.1 M sodium phosphate buffer (pH 7.0) solution containing 0.1 M $LiClO_4$. The catalytic process found at a potential of +1150 mV (Figure S5, Supporting Information) is about 50 mV more positive than that observed with the thick-film $[Ru^{II}bpy]_5[Ru^{III}_4POM]$ modified GC electrode under the same conditions (Figure 5b). Consequently, $[Ru^{II}bpy]_5[Ru^{III}_4POM]$ was chosen for quantitative studies, described below, instead of $[Ru^{II}bpy]_4[Ru^{IV}_4POM]$, for the reasons of better stability and lower overpotential for catalytic electrooxidation of water. However, before these results are presented, a brief report on the absence of catalytic activity of related compounds is provided.

Voltammetry of Thick-Film $[Ru^{II}bpy]_2[POM]$ (POM = $[S_2W_{18}O_{62}]^{4-}$ and $[S_2Mo_{18}O_{62}]^{4-}$) Modified Electrodes in 0.1 M Sodium Phosphate Buffer (pH 7.0) with 0.1 M $LiClO_4$ as an Additional Electrolyte. To establish the important role of the $[Ru^{III}_4POM]$ in the mechanism for the catalytic water oxidation, we studied the $[Ru^{II}bpy]$ salts of $[S_2W_{18}O_{62}]^{4-}$ and $[S_2Mo_{18}O_{62}]^{4-}$ polyoxometalates, where again the POMs themselves cannot be oxidized. As can be seen from the oxidation shown in Figure 7, within the positive potential window available in the aqueous electrolyte media, the major voltammetric response for $[Ru^{II}bpy]_2[S_2Mo_{18}O_{62}]$ and $[Ru^{II}bpy]_2[S_2W_{18}O_{62}]$ modified electrodes involves $[Ru(bpy)_3]^{2+/3+}$ redox chemistry. In the case of the thick-film $[Ru^{II}bpy]_2[S_2Mo_{18}O_{62}]$ modified electrode, the fact that the voltammetric response associated with the $[Ru(bpy)_3]^{2+/3+}$ process is not fully reversible suggests that catalytic water oxidation may occur via the $[Ru^{III}bpy]$. However, the peak current is significantly smaller than that found in the thick-film $[Ru^{II}bpy]_5[Ru^{III}_4POM]$ case, and no bubbles of gas were visually observed when the potential was held at 1.3 V. Moreover, RRDE experiments failed to detect oxygen (vide infra). With the thick-film $[Ru^{II}bpy]_2[S_2W_{18}O_{62}]$ modified electrode, there is no evidence for oxygen formation from the voltammetric perspective, because the $[Ru(bpy)_3]^{2+/3+}$ process exhibits reversible characteristics. Tests with thick-film $([Ru^{II}bpy]_5[S_2M_{18}O_{62}]_2$ (M = Mo and W) electrodes, where $[S_2M_{18}O_{62}]^{5-}$ is the one-electron reduced form of $[S_2M_{18}O_{62}]^{4-}$, also showed no detectable catalytic activity (RRDE analysis) toward water oxidation. This is as expected because $[S_2M_{18}O_{62}]^{5-}$ is converted into $[S_2M_{18}O_{62}]^{4-}$ in the positive potential region. Therefore, use of $[Ru^{II}bpy]_5[S_2M_{18}O_{62}]_2$ modified electrode is effectively the same as a $[Ru^{II}bpy]_2[S_2M_{18}O_{62}]$ one, although the reduced form is expected to be less water-soluble. These results support the hypothesis that it is the $[Ru^{III}_4POM]$ component of $[Ru^{II}bpy]_5[Ru^{III}_4POM]$ complex that contains the catalytically active component, while $[Ru^{III}bpy]$ acts solely as an electron transfer mediator.

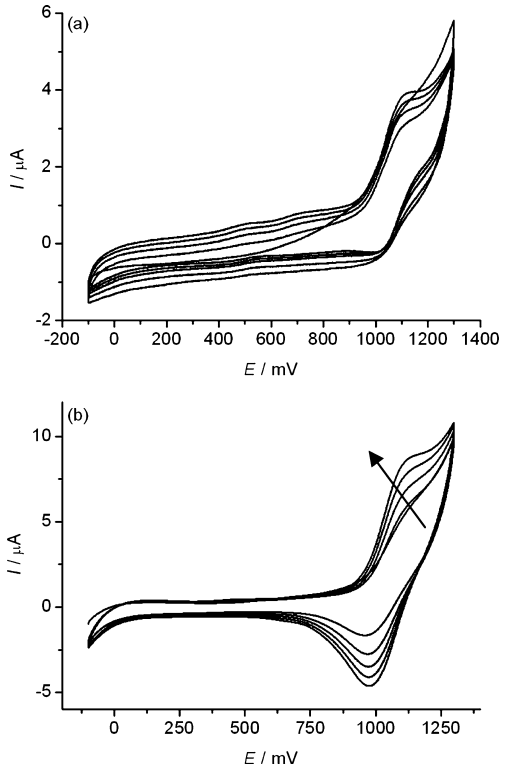

Figure 7. Cyclic voltammograms from thick-film (a) $[Ru^{II}bpy]_2[S_2Mo_{18}O_{62}]$ and (b) $[Ru^{II}bpy]_2[S_2W_{18}O_{62}]$ modified electrodes with 0.1 M sodium phosphate buffer (pH 7.0) containing 0.1 M $LiClO_4$ as the additional supporting electrolyte. Scan rate: 50 mV s^{-1}.

Voltammetry of $[Fe^{II}Phen]_x[Ru^{III}_4POM]$ Material ($[Fe^{II}Phen]$ = Iron Phenanthroline) Thick-Films in 0.1 M Sodium Phosphate Buffer (pH 7.0) with 0.1 M $LiClO_4$ as an Additional Supporting Electrolyte. The cationic electron transfer mediator iron phenanthroline was also used to form water insoluble complexes with $[Ru^{III}_4POM]$, using analogous procedures developed for synthesis of $[Ru^{II}bpy]_5[Ru^{III}_4POM]$. Tris(phenanthroline)iron(II), $[Fe^{II}Phen]$, has been used as a redox mediator in other studies and has a standard reversible potential of +860 mV (vs Ag/AgCl).[20] Consequently, $[Fe^{III}Phen]$, in principle, is thermodynamically capable of generating $[Ru^{V}_2Ru^{IV}_2POM]$, based on the reversible potential data,[7] but not the more oxidized form of the catalyst needed for turnover. The electrochemistry of $[Fe^{II}Phen]_x[Ru^{III}_4POM]$ was investigated in 0.1 M sodium phosphate buffer (pH 7.0) containing 0.1 M $LiClO_4$ as the additional electrolyte. A voltammogram derived from this $[Fe^{II}Phen]_x[Ru^{III}_4POM]$ modified GC electrode is shown in Figure 8. The oxidation process having a reversible potential of +890 mV is assigned to the $Fe^{2+/3+}$ process derived from oxidation of $[Fe^{II}Phen]$. No gas bubble formation was observed, and RRDE experiments show no detectable oxygen. These results, along with retention of reversibility, imply that $[Fe^{II}Phen]$ is not a good electron transfer mediator, probably because its oxidized Fe^{3+} form is not a strong enough oxidant to generate the catalytically active $[Ru^{V}_4POM]$.

Quantitative Detection of Oxygen Generated by Water Oxidation at a $[Ru^{II}bpy]_5[Ru^{III}_4POM]$ Modified

dx.doi.org/10.1021/ic500878w | Inorg. Chem. 2014, 53, 7561−7570

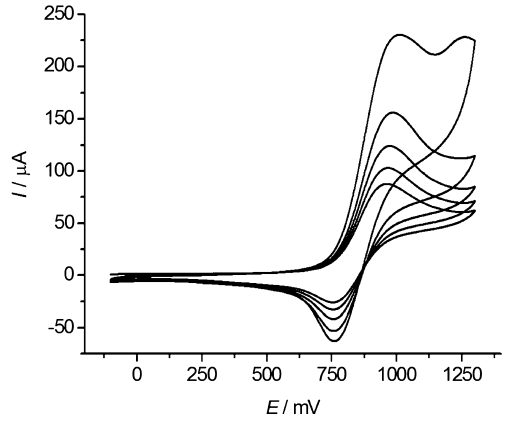

Figure 8. Cyclic voltammograms from $[Fe^{II}Phen]_x[Ru^{III}{}_4POM]$ thick-film modified electrode in 0.1 M sodium phosphate buffer (pH 7.0) containing 0.1 M $LiClO_4$ as the additional supporting electrolyte. Scan rate: 50 mV s^{-1}.

Glassy Carbon Electrode Using the RRDE Method. In cyclic voltammetric studies with $[Ru^{II}bpy]_5[Ru^{III}{}_4POM]$ modified electrodes, bubbles were observed to form on the modified electrode surface when the potential was sufficiently positive. This implies that oxygen is generated by catalytic oxidation. In order to identify and quantify the amount of oxygen generated, a rotating ring disk (Pt collection ring, glassy carbon generation disk) electrode (RRDE), where the glassy carbon disk was modified with $[Ru^{II}bpy]_5[Ru^{III}{}_4POM]$, was used. The oxygen reduction process is complex. To use the RRDE method quantitatively, the mechanism for O_2 reduction at the Pt electrode used under the relevant experimental conditions needs to be known, as does the collection efficiency of the RRDE electrode.

Oxygen Reduction at the Pt RDE. Because the nature of oxygen reduction is strongly dependent on the electrolyte and electrode material,[26] the mechanism applicable under conditions where oxygen is produced in the catalytic water oxidation process needs to be known. A platinum RDE electrode was used to measure the number of electrons involved in oxygen reduction in an air saturated solution of 0.1 M phosphate buffer (pH 7.0) containing 0.1 M $LiClO_4$ as an additional supporting electrolyte. Data obtained with the platinum electrode using rotation rates over the range 52.4 to 314.2 rad s^{-1} were examined. The limiting current is only proportional to the square root of the angular frequency over rotation rates of 52.4 to 157.0 rad s^{-1}, which is expected if the process is controlled by mass transport. This linear relationship breaks down when the rotation rate is above 157.0 rad s^{-1} and O_2 reduction kinetics becomes rate-limiting. To ensure calibration is undertaken in the mass-transport-controlled regime, we used rotation rates of 52.4, 104.7, and 157.0 rad s^{-1} for the estimation of the number of electrons involved in O_2 reduction and the Levich equation. A value of 0.25 mM was used for the oxygen concentration in air-saturated water.[27] Assuming the diffusion coefficient of oxygen dissolved in water is 2.0×10^{-5} cm^2 s^{-1},[28] the number of electrons involved in the reduction process was calculated to be n = 3.6 (±0.1). It is therefore concluded that four electrons are involved in oxygen reduction in an aqueous buffer solution (pH 7.0) at the platinum electrode and that the overall process is postulated to be $O_2 + 4e^- + 4H^+ \rightarrow 2H_2O$.

Detection of Oxygen at a $[Ru^{II}bpy]_5[Ru^{III}{}_4POM]$ Modified GC Disk Using RRDE. The quantity of oxygen generated during the catalytic water oxidation at both thick- and thin-film $[Ru^{II}bpy]_5[Ru^{III}{}_4POM]$ modified electrodes was determined by the RRDE method. Because $[Ru^{II}bpy]_5[Ru^{III}{}_4POM]$ did not adhere very well to the smooth GC electrode under RRDE hydrodynamic conditions, film adhesion was improved by coating the modified surface with a thin Nafion film (see the Experimental Section for details) to prevent detachment of $[Ru^{II}bpy]_5[Ru^{III}{}_4POM]$. Introduction of the Nafion film caused a decrease of 15% in the oxidation peak current under stationary electrode conditions, attributed to some catalytically active sites being blocked by the Nafion. During RRDE measurements, the disk electrode potential was scanned from +300 to +1400 mV for the thin film case (or +1200 mV for the thick-film case) at a rate of 50 mV s^{-1}. A constant potential of −300 mV applied to the ring electrode was selected as being appropriate to reduce the oxygen after it was swept to the ring electrode, subsequent to generation at the modified GC electrode. The electrode reactions taking place at the disk and ring electrodes are assumed to be the following for the forward (positive potential direction) scan:

Reaction at disk electrode:

$$2H_2O \rightarrow O_2 + 4H^+ + 4e^- \quad (13)$$

Reaction at ring electrode:

$$O_2 + 4e^- + 4H^+ \rightarrow 2H_2O \quad (14)$$

From Figure 9a, an oxygen reduction current of −5.2 μA was measured at the ring electrode when the potential at the thin-film modified disk reached +1100 mV. The voltammetric response at the disk was independent of rotation rate, which implies that the catalytic water oxidation reaction is kinetically limited.[17] As a consequence, the TOF of the catalyst, defined as the moles of O_2 produced per mole of POM per second, can be calculated from the oxygen reduction current at the ring electrode, I_R, using the following relationship,[15]

$$\mathrm{TOF} = \frac{-I_R}{n_R F A N_{CL} \Gamma} \quad (15)$$

where n_R is the number of electrons transferred per oxygen molecule at the ring electrode, F is Faraday's constant, A is the area of the disk electrode, Γ is the surface concentration of the catalyst, and N_{CL} is the collection efficiency. Because the surface concentration of $[Ru^{II}bpy]_5[Ru^{III}{}_4POM]$ for the thin-film case was calculated to be 7.4×10^{-10} mol cm^{-2}, on the basis of the known amount of $[Ru^{II}bpy]_5[Ru^{III}{}_4POM]$ cast onto the electrode surface (see the Experimental Section for details), a TOF value of 0.35 s^{-1} was obtained at +1.10 V. Analogously, a TOF value of 1.6×10^{-2} s^{-1} was obtained at +1.15 V when the thick-film modified electrode was used (Figure 9b). It should be noted that the ring current due to $4e^-$ reduction of O_2 is considerably smaller than expected on the basis of the disc current for the $4e^-$ O_2 evolution process and the known collection efficiency of 0.42, which suggests that not all anodic processes ultimately result in O_2 production, presumably because some $[Ru^{II}bpy]_5[Ru^{III}{}_4POM]$ material is buried inside the film. The fact that the Faraday efficiency is larger under the thin-film condition (0.28 vs 0.18, estimated on the basis of eq 16[29]) confirms that use of the thin-film configuration is desirable.

dx.doi.org/10.1021/ic500878w | Inorg. Chem. 2014, 53, 7561−7570

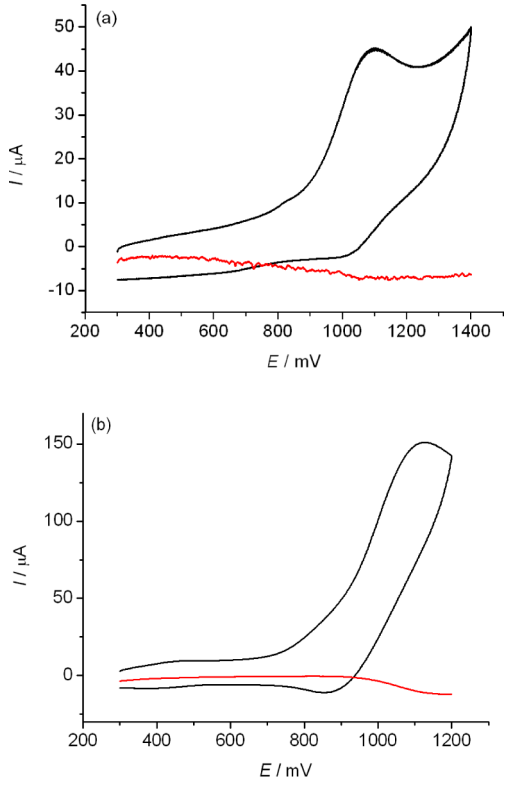

Figure 9. Detection of O_2 generated during catalytic water oxidation when (a) thin- and (b) thick-film $[Ru^{II}bpy]_5[Ru^{III}{}_4POM]$ modified RRDEs are in contact with 0.1 M phosphate buffer (pH 7.0) containing 0.1 M $LiClO_4$ as the additional electrolyte. At the disk electrode (black line), the potential was scanned from +300 to +1200 or 1400 mV at a rate of 50 mV s^{-1}; at the ring electrode (red line), the potential applied was −300 mV. Rotation rate: 104.7 rad s^{-1}.

$$\text{Faradaic efficiency} = \left| \frac{I_R n_D}{N_{CL} I_D n_R} \right| \quad (16)$$

(where n_D is the number of electrons transferred per oxygen molecule generation at the disk electrode, which is 4, as suggested by eq 13, and I_D stands for the disk current.)

Control experiments were also carried out using a bare RRDE placed in contact with 0.1 M phosphate buffer (pH 7.0) containing 0.1 M $LiClO_4$ and at a $[Ru^{II}bpy]_5[Ru^{III}{}_4POM]$ modified RRDE placed in contact with 0.5 M H_2SO_4 using otherwise identical conditions. No oxygen was detected at the platinum ring electrode in either case. This confirms that the reduction current detected at the platinum ring electrode when the disk electrode was modified with $[Ru^{II}bpy]_5[Ru^{III}{}_4POM]$ was derived from reduction of oxygen generated by the oxidation of water catalyzed by $[Ru^{II}bpy]_5[Ru^{III}{}_4POM]$. O_2 also was undetectable at the ring electrode when the electrodes were modified with thick-films of $[Ru^{II}bpy]_2[S_2W_{18}O_{62}]$, $[Ru^{II}bpy]_2[S_2Mo_{18}O_{62}]$, and $[Fe^{II}Phen]_x[Ru^{III}{}_4POM]$ materials.

Comparison with Literature Data on Other Systems. Several examples of TOF values reported for catalytic electrochemical water oxidation are given in Table 1. The $[Ru^{II}bpy]_5[Ru^{III}{}_4POM]$ thin-film modified electrode used in this study shows an order of magnitude higher TOF at ∼0.49 V overpotential than when $[\{Ru^{IV}{}_4O_4(OH)_2(H_2O)_4\}(\gamma\text{-}SiW_{10}O_{36})_2]^{10-}$ anion was attached to a multiwall carbon nanotube (MWCNT) modified electrode at pH 7.0.[7] However, the TOF value is still well below the ≥6 s^{-1} value per iridium site reported by Murray and coauthors[15,30] when using either dissolved IrO_x nanoparticles or a IrO_x film as the catalyst for water oxidation, albeit with a higher overpotential of ≥0.69 V. Furthermore, the value of 6.6 s^{-1} per mole of IrO_2 with an overpotential of 0.58 V at pH 5.8 reported by Yagi and coauthors[31] is higher than the 0.26 s^{-1} value obtained at a dendron functionalized graphene at a higher overpotential of 0.6 V[9] but not quite as high as the value of 0.82 s^{-1} reported at a graphene modified electrode at an overpotential of 0.35 V in a pH 7.5 buffer with 1 M $Ca(NO_3)_2$ as the additional electrolyte.[10]

CONCLUSIONS

A water insoluble compound, $[Ru^{II}bpy]_5[Ru^{III}{}_4POM]$, has been synthesized and used to modify GC electrodes under thin- and thick-film conditions. The results imply that $[Ru^{II}bpy]_5[Ru^{III}{}_4POM]$ facilitates efficient water oxidation, particularly under thin-film modified electrode conditions, where $[Ru^{III}bpy]$ acts as the electron transfer mediator and $[Ru^{V}{}_4POM]$ is the O_2-releasing form of the catalyst. TOF data imply that combining the electron transfer mediator and the catalyst into a single complex provides greatly improved catalytic water oxidation efficiency by this tetra-ruthenium POM. Thus, the turnover frequency of 0.35 s^{-1} achieved at the low overpotential of 0.49 V at the thin-film modified electrode is much higher than reported for the same catalyst using MWCNT[8] or dendron-functionalized graphene[9] approaches, but not as high as that found at a graphene modified electrode.[10] The mechanism of mediator enhanced catalytic water oxidation process is believed to be associated with the sequence of reactions given in eqs 11 and 12.

Table 1. Comparison of Data Available with Other Systems

system	pH	overpotential (V)	TOF (s^{-1})	reference
$[Ru^{II}bpy]_5[Ru^{III}{}_4POM]$	7.0	0.49	0.35 (thin-film)	this work
		0.54	0.016 (thick-film)	
POM @ MWCNT	7.0	0.35	0.01	8
POM @ MWCNT	7.0	0.48	0.028	8
POM @ MWCNT	7.0	0.55	0.055	8
POM @ MWCNT	7.0	0.60	0.085	8
POM @ dendron-graphene	7.0	0.60	0.26	9
POM @ graphene	7.5	0.35	0.82	10
dissolved IrO_x	13	0.74	8−11	30
IrO_x film	7.0	0.69	6.0	14
IrO_2 film	5.3	0.58	6.6	31

dx.doi.org/10.1021/ic500878w | Inorg. Chem. 2014, 53, 7561−7570

■ ASSOCIATED CONTENT

Supporting Information

Simulated voltammogram supporting the mechanism proposed for the cyclic voltammetric responses of $[Ru^{II}bpy]_5[Ru^{III}{}_4POM]$ modified electrodes in an aqueous 0.5 M H_2SO_4 solution. Cyclic voltammogram obtained with a thick-film $[Ru^{II}bpy]_4[Ru^{IV}{}_4POM]$ modified GC electrode in 0.5 M H_2SO_4. Cyclic voltammogram obtained at a RuO_2 modified glassy carbon electrode (fabricated using drop casting method with 5 μL of 1 mg mL^{-1} RuO_2) in contact with 0.1 M sodium phosphate buffer (pH 7.0) containing 0.1 M $LiClO_4$. Cyclic voltammograms derived from thick-film $[Ru^{II}bpy]_4[Ru^{IV}{}_4POM]$ modified GC electrodes with 0.1 M sodium phosphate buffer (pH 7.0) containing 0.1 M $LiClO_4$ as the additional electrolyte. This material is available free of charge via the Internet at http://pubs.acs.org.

■ AUTHOR INFORMATION

Corresponding Authors

*E-mail: jie.zhang@monash.edu.
*E-mail: alan.bond@monash.edu.
*E-mail: chill@emory.edu.

Notes

The authors declare no competing financial interest.

■ ACKNOWLEDGMENTS

J.Z. and A.M.B. would like to thank the Australian Research Council for financial support. C.L.H. thanks the National Science Foundation (Grants CHE-1124862 and CHE-0911610) for support.

■ REFERENCES

(1) (a) Cady, C. W.; Crabtree, R. H.; Brudvig, G.W. *Coord. Chem. Rev.* **2008**, *252*, 444−455. (b) Dismukes, G. C.; Brimblecombe, R.; Felton, G. A. N.; Pryadun, R. S.; Sheats, J. E.; Spiccia, L.; Swiegers, G. F. *Acc. Chem. Res.* **2009**, *42*, 1935−1943. (c) Dau, H.; Zaharieva, I. *Acc. Chem. Res.* **2009**, *42*, 1861−1870. (d) Penner-Hahn, J. E.; Yocum, C. F. *Science* **2005**, *310*, 982−983.

(2) Geletii, Y. V.; Yin, Q.; Hou, Y.; Huang, Z.; Ma, H.; Song, J.; Besson, C.; Luo, Z.; Cao, R.; O'Halloran, K. P.; Zhu, G.; Zhao, C.; Vickers, J. W.; Ding, Y.; Mohebbi, S.; Kuznetsov, A. E.; Musaev, D. G.; Lian, T.; Hill, C. L. *Isr. J. Chem.* **2011**, *51*, 238−246.

(3) (a) Hill, C. L. *Chem. Rev.* **1998**, *98*, 389−390. (b) Long, D.; Burkholder, E.; Cronin, L. *Chem. Soc. Rev.* **2007**, *36*, 105−121.

(4) Geletii, Y. V.; Botar, B.; Kögerler, P.; Hillesheim, D. A.; Musaev, D. G.; Hill, C. L. *Angew. Chem., Int. Ed.* **2008**, *47*, 3896−3899.

(5) Geletii, Y. V.; Besson, C.; Hou, Y.; Yin, Q.; Musaev, D. G.; Quiñonero, D.; Cao, R.; Hardcastle, K. I.; Proust, A.; Kögerler, P.; Hill, C. L. *J. Am. Chem. Soc.* **2009**, *131*, 17360−17370.

(6) Sartorel, A.; Carraro, M.; Scorrano, G.; Zorzi, R. D.; Geremia, S.; McDaniel, N. D.; Bernhard, S.; Bonchio, M. *J. Am. Chem. Soc.* **2008**, *130*, 5006−5007.

(7) (a) Lee, C. Y.; Guo, S.-X.; Murphy, A. F.; McCormac, T.; Zhang, J.; Bond, A. M.; Gueletii, Y. V.; Zhu, G.; Hill, C. L. *Inorg. Chem.* **2012**, *51*, 11521−11532. (b) Liu, Y.; Guo, S. X.; Bond, A. M.; Zhang, J. *Inorg. Chem.* **2013**, *52*, 11986−11996.

(8) Toma, F. M.; Sartorel, A.; Iurlo, M.; Carraro, M.; Parisse, P.; Maccato, C.; Rapino, S.; Gonzalez, B. R.; Amenitsch, H.; Ros, T. D.; casalis, L.; Goldoni, A.; Marcaccio, M.; Scorrano, G.; Scoles, G.; Paolucci, F.; Prato, M.; Bonchio, M. *Nat. Chem.* **2010**, *2*, 826−831.

(9) Quintana, M.; Lopez, A. M.; Rapino, S.; Toma, F. M.; Iurlo, M.; Carraro, M.; Sartorel, A.; Maccato, C.; Ke, X. X.; Bittencourt, C.; Da Ros, T.; Van Tendeloo, G.; Marcaccio, M.; Paolucci, F.; Prato, M.; Bonchio, M. *ACS Nano* **2013**, *7*, 811−817.

(10) Guo, S.-X.; Liu, Y.; Lee, C.-Y.; Bond, A. M.; Zhang, J.; Geletii, Y. V.; Hill, C. L. *Energy Environ. Sci.* **2013**, *6*, 2654−2663.

(11) Wang, J. *Chem. Rev.* **2007**, *108*, 814−825.

(12) Anson, F. C.; Ni, C. L.; Saveant, J. M. *J. Am. Chem. Soc.* **1985**, *107*, 3442−3450.

(13) (a) Hultgren, V. M.; Bond, A. M.; Wedd, A. G. *Dalton Trans.* **2001**, *7*, 1076−1082. (b) Keyes, T. E.; Gicquel, E.; Guerin, L.; Forster, R. J.; Hultgren, V.; Bond, A. M.; Wedd, A. G. *Inorg. Chem.* **2003**, *42*, 7897−7905. (c) Zhang, J.; Goh, J.-K.; Tan, W.-T.; Bond, A. M. *Inorg. Chem.* **2006**, *45*, 3732−3740.

(14) Fay, N.; Hultgren, V. M.; Wedd, A. G.; Keyes, T. E.; Forster, R. J.; Leane, D.; Bond, A. M. *Dalton Trans.* **2006**, 4218−4227.

(15) Albery, W. J.; Hitchman, M. L. *Ring-Disc Electrodes*; Clarendon Press: Oxford, 1971.

(16) Nakagawa, T.; Beasley, C. A.; Murray, R. W. *J. Phys. Chem. C* **2009**, *113*, 12958−12961.

(17) Sawyer, D. T.; Sobkowiak, A.; Roberts, J. L., Jr. *Electrochemistry for Chemists*, 2nd ed.; Wiley: New York, 1995.

(18) Bard, A. J.; Faulkner, L. R. *Electrochemical Methods: Fundamentals and Applications*, 2nd ed.; Wiley: New York, 2001.

(19) *DigiSim for Windows 95*, version 3.05; Bioanalytical Systems, Inc.: West Lafayette, IN, 2000.

(20) Ma, H.; Shi, S.; Zhang, Z.; Pang, H.; Zhang, Y. *J. Electroanal. Chem.* **2010**, *648*, 128−133.

(21) Bard, A. J.; Fan, F.-R. F.; Mirkin, M. V. In *Electroanalytical Chemistry*; Bard, A. J., Ed.; Marcel Dekker: New York, 1994; Vol. *18*, pp 243−373.

(22) Zhang, J.; Bond, A. M.; Belcher, J.; Wallace, K. J.; Steed, J. W. *J. Phys. Chem. B* **2005**, *107*, 5777−5786.

(23) (a) Stracke, J. J.; Finke, R. G. *J. Am. Chem. Soc.* **2011**, *133*, 14872−14875. (b) Hocking, R.; Brimblecombe, R.; Chang, L.; Singh, A.; Cheah, M.; Glover, C.; Casey, W.; Spiccia, L. *Nat. Chem.* **2011**, *3*, 461−466.

(24) (a) Mills, A. *Chem. Soc. Rev.* **1989**, *18*, 285−316. (b) Lee, Y.; Suntivich, J.; May, K. J.; Perry, E. E.; Yang, S.-H. *J. Phys. Chem. Lett.* **2012**, *3*, 399−404. (c) Mamaca, N.; Mayousse, E.; Arrii-Clacens, S.; Napporn, T. W.; Servat, K.; Guillet, N.; Kokoh, K. B. *Appl. Catal., B* **2012**, *111− 112*, 376−380.

(25) Lee, C. Y.; Bond, A. M. *Langmuir* **2010**, *26*, 16155−16162.

(26) Zhang, J., Ed. *PEM Fuel Cell Electrocatalysts and Catalyst Layers: Fundamentals and Applications*; Springer: London, 2008.

(27) Chan, C.; Lehmann, M.; Chan, K.; Chan, P.; Chan, C.; Gruendig, B.; Kunze, G.; Renneberg, R. *Biosens. Bioelectron.* **2000**, *15*, 343−353.

(28) Lorbeer, P.; Lorenz, W. J. *Electrochim. Acta* **1980**, *25*, 375 and references therein.

(29) Liu, Y. P.; Guo, S. X.; Bond, A. M.; Zhang, J.; Du, S. W. *Electrochim. Acta* **2013**, *101*, 201−208.

(30) Nakagawa, T.; Bjorge, N. S.; Murray, R. W. *J. Am. Chem. Soc.* **2009**, *131*, 15578−15579.

(31) (a) Yagi, M.; Tomita, E.; Sakita, S.; Kuwabara, T.; Nagai, K. *J. Phys. Chem. B* **2005**, *109*, 21489. (b) Kuwabara, T.; Tomita, E.; Sakita, S.; Hasegawa, D.; Sone, K.; Yagi, M. *J. Phys. Chem. C* **2008**, *112*, 3774−3779.